An Investigation on Friction Factors and Heat Transfer Coefficients in a Rectangular Duct with Surface Roughness

Soo Whan Ahn*, Kang Pil Son
School of Transport Vehicle Engineering, Institute of Marine Industry, Gyeongsang National University, #445 Inpyong-dong, TongYong, Kyongnam 650-160, Korea

An investigation on the fully developed heat transfer and friction factor characteristics has been made in rectangular ducts with one-side roughened by five different shapes. The effects of rib shape geometries as well as Reynolds numbers are examined. The rib height-to-duct hydraulic diameter, pitch-to-height ratio, and aspect ratio of channel width to height are fixed at e/De=0.0476, P/e=8, and W/H=2.33, respectively. To understand the characteristics of heat transfer enhancements, the friction factors are also measured. The data indicates that the triangular type rib has a substantially higher heat transfer performance than any other ones.

Key Words : Heat Transfer Coefficient, Pressure Drop, Rib-Roughened Rectangular Duct, Heat Transfer Performance, Roughness Function

Nomenclature

AR : Aspect ratio of channel width to height
De : Hydraulic diameter (m)
e : Roughness height (m)
e^+ : Roughness Reynolds number, $(e/De)\,Re(f/2)0.5$
f : Average friction factor for the channel volume
f_r : Friction factor based on the rough wall
H : Duct height (m)
Nu : Nusselt number
ΔP : Pressure difference (Pa)
P : Roughness pitch (m)
Re : Reynolds number, $(u_b\,De)/\nu$
St : Stanton number, $Nu/(Re\,P_r)$
T_b : Bulk temperature (K)
T_w : Wall temperature (K)
U : Local velocity (m/s)
U^* : Friction velocity (m/s)
u_b : Bulk velocity (m/s)
W : Duct width (m)
ν : Kinematic viscosity (m^2/s)

* Corresponding Author,
E-mail : swahn@gaechuk.gsnu.ac.kr
TEL : +82-55-640-3125; **FAX** : +82-55-640-3128
School of Transport Vehicle Engineering, Institute of Marine Industry, Gyeongsang National University, #445 Inpyong-dong, TongYong, Kyongnam 650-160, Korea.
(**Received** May 19, 2001; **Revised** December 21, 2001)

1. Introduction

A well-known method to increase the heat transfer from a surface is to roughen the surface either randomly with a sand grain or by use of regular geometric roughness elements on the surface. However, the increase in heat transfer is accompanied by an increase in resistance to fluid flow. Many investigators have studied this problem in an attempt to develop accurate predictions of the behaviour on a given roughness geometry and to define a geometry which gives the best transfer performance for a given flow friction. An early study of the effect of roughness on friction factor and velocity distribution was performed by Nikuradse (1933), who conducted a series of experiments with pipes roughened by sand grains. One of first studies on the heat transfer in rough tubes was conducted by Cope (1941), and a very thorough study with two dimensional roughness elements by Nunner (1958). A number of friction and heat transfer measurements have been performed for repeated-

rib roughness in the rectangular duct flow, such as Hwang (1998), Han et al. (1978), and Kwon et al. (2000). Hwang (1998) investigated the fully developed heat transfer characteristics in the rectangular ducts with one wall roughened by slit and solid ribs. He concluded that the slit-ribbed geometry yielded higher heat transfer coefficients than the solid-ribbed geometry because of the greater turbulence mixing effects. Furthermore, slit ribs with larger void fractions in a lower Reynolds number range provided better thermal performance under a constant power constraint. The effects of rib shape, angle of attack, and pitch to height ratio on friction factors and heat transfer coefficients in a parallel plate with rib-roughened surfaces were studied by Han et al. (1978). They showed that ribs at a 45° angle of attack yielded superior heat transfer performance for a given power when compared to ribs at a 90° angle of attack or to a sand-grain roughness. Kwon et al. (2000) studied the influence of arrangement and length of discrete ribs on heat/mass transfer and friction loss in a rectangular duct.

However, there are little research on rib shape in the channel flow. Recently, Arman and Rabas (1992) predicted the effect of the rib shape on the Nusselt number and friction factor in a circular tube. The numerical model was validated by predicting the heat transfer coefficients and friction factors of the two-dimensional roughness geometries by Hijikata and Mori (1987). Investigating the effect of four different rib shapes such as semicircle, sine, trapezoid, and arc, they reported that the increases in the heat transfer were in the order of arc, semicircle, sine, and trapezoid. The objective of present study is to investigate the effects of rib shapes on the heat transfer and friction in a rectangular channel. Measurements on the five different rib shapes; i.e. square, triangle, circle, semicircle, and arc were made. The channel width-to-height ratio was 2.33. The rib pitch-to-height ratio (P/e) and the rib height-to-hydraulic diameter ratio (e/De) were 8 and 0.0476, respectively. The centerline friction factors and heat transfer coefficient distribution on the bottom ribbed wall were measured. The smooth rectangular channel was also checked out for a reference.

2. Experimental Studies

A schematic diagram of the experimental apparatus is shown in Fig. 1. A 0.86kW blower forced air through the test channel. The test channel was constructed by using acrylic plates (5mm thickness) and aluminum plates (5mm thickness). A 70(W) mm×30(H) mm rectangular duct with a 3600mm length was fabricated. The rib pitch-to-height ratio (P/e) and the rib height-to-hydraulic diameter ratio (e/De) were 8 and 0.0476, respectively. The aluminum ribs were glued onto the bottom plates of the channels.

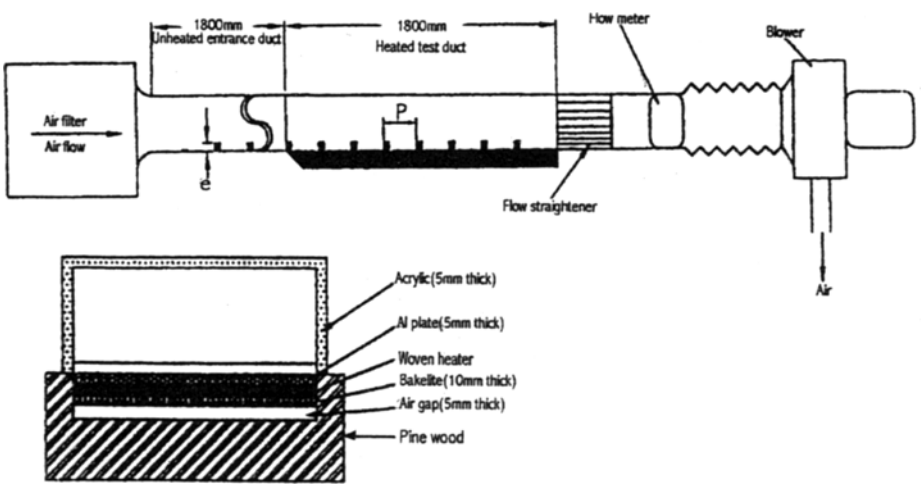

Fig. 1 Schematic diagram of experimental setup

As given in Fig. 1, the lower horizontal wall of the test section is heated and remaining walls are thermally insulated. Upstream of the test duct is an unheated roughened entrance section. This unheated duct provides a hydrodynamically fully developed condition at the entrance of the heated test channel. The heated surface, as shown schematically in Fig. 1, is constructed using aluminum segments. The surface of the aluminum plate and ribs are highly polished to minimize emissivity, hence radiative losses. In order to check out the effects of rib shape, the different type ribs were sequentially installed on the plate shown in Fig. 2. In the entire channel length, 1,800mm of the bottom plate was soley heated by a woven heater (HTWC, OMEGA Co.). The heater could be independently controlled by a variac transformer, which provided a controllable constant heat flux for the test plate. The woven heaters embedded in silicone rubber were clamped uniformly between a bakelite panel and the aluminum plate with the high thermally conductive epoxy adhesive (Omegabond 400, OMEGA Co.) to insure good contact. The heater could provide a constant heat flux for entire test surface using the watt meter. The blower (0.8kW, 3,4000rpm, A/C motor) was capable of providing a wide range of air velocities so that the Reynolds number could be varied between 10,000 and 70,000. The pressure drop across the test

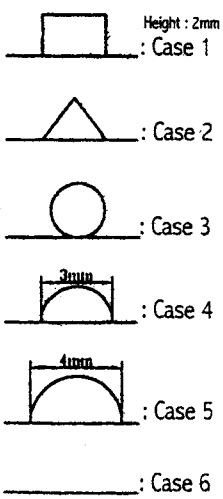

Fig. 2 Rib shape

section was measured by a micro-manometer (FCO-12) calibrated by the inclined manometer. A total of 16 pressure taps with static pitot tubes were installed along the spanwise centerline of the bottom aluminum plate for local static wall pressure measurements. The static pitot tube in the tap was connected to a micro-differential transducer with accuracy up to 0.3mm of water to amplify the pressure signals, which were subsequently transferred to a digital readout. The time to reach steady state was less than 60 minutes. Over the range of test conditions, the wall-to-bulk fluid temperature difference varied between 10℃ and 32℃. Since the turbulence generated by ribs tended to be dominant over the secondary flow generated by buoyancy forces, the influence of free convection on the heat transfer was believed to be negligible. To minimize the conductive heat loss, the backside surface of the bakelite board was insulated using a 15 mm thick section of pine wood with a 5 mm thick clearance (air gap) between them as in Fig. 1. The floor surface was instrumented with eighteen thermocouples. The junction-beads of the thermocouples were carefully embedded into the wall and then grounded flat to ensure that they are flush with the surfaces. In addition, a thermocouple probe and a thermocouple rake were placed at the test duct inlet and exit, respectively, for airflow temperature measurements. The temperature signals were transferred to a hybrid recorder, and subsequently sent to a computer. The fully developed average heat transfer coefficients for the rectangular ducts were determined by the ratio of the floor heat flux to the difference between the floor and air bulk mean temperature:

$$h=Q_{net}/[A(T_w-T_b)] \tag{1}$$

where the heat transfer area (A) wes always that of the smooth bottom wall. Q_{net} was the electrical power generated from a heater subtracted from the heat loss to the outside of the test channel and it was calculated based on the following energy balance equation:

$$Q_{net}=Q_t-Q_c-Q_r \tag{2}$$

where Q_t was the total power input to the test

section, Q_c the conduction heat loss to the environment, Q_r the radiative heat loss from the roughened surface to its surroundings. Heat loss from the outside of the duct wall through the bakelite to pine wood was quite low (about 0.5 percent for the maximum). The value of Q_r was evaluated using a diffusive gray-surface network (Siegel and Howell, 1981), and the loss due to radiation was less than 1.5 percent of total power input. The bulk temperature (T_b) was calculated from the following equation:

$$T_b=\frac{Q_{net}}{A_c u_b C_p \rho_{air}}+T_{air} \quad (3)$$

where A_c and u_b were the channel cross sectional area and bulk velocity, respectively. The ambient temperature (T_{air}) was about 23℃. From Eq. (1), the Nusselt number (Nu) is given by:

$$Nu=\frac{hDe}{k} \quad (4)$$

where k means the thermal conductivity. The average friction factor for the whole channel was calculated from the average static pressure drop difference across the flow channel (ΔP) and the mass flow rate of the air (G) as:

$$f=\Delta P/[4(L/De)[G^2/2\rho]] \quad (5)$$

The average static pressure drop difference across the flow channel was measured with series of static pitot tubes. A conservative estimate of the accuracy of the temperature measurement was ±1℃. The heat flux was measured by the watt meter with a maximum uncertainty of ±3.2%. The uncertainty associated with the length scale used in the data reduction was ±2mm. It was found that, for the minimum flow rate, which was the worst case, the uncertainties for Nusselt number, Reynolds number and friction factor were ±9.5, ±6.5 and ±8.5%, respectively. The uncertainty estimate procedure was described by Kline and McClintock (1953).

3. Results and Discussion

Prior to ribbed duct experiments, the fully developed friction factors and heat transfer coefficients were measured for a smooth duct

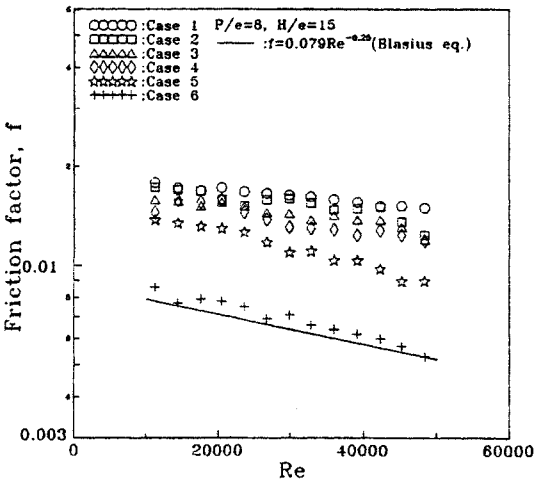

Fig. 3 Average friction factor for whole channel

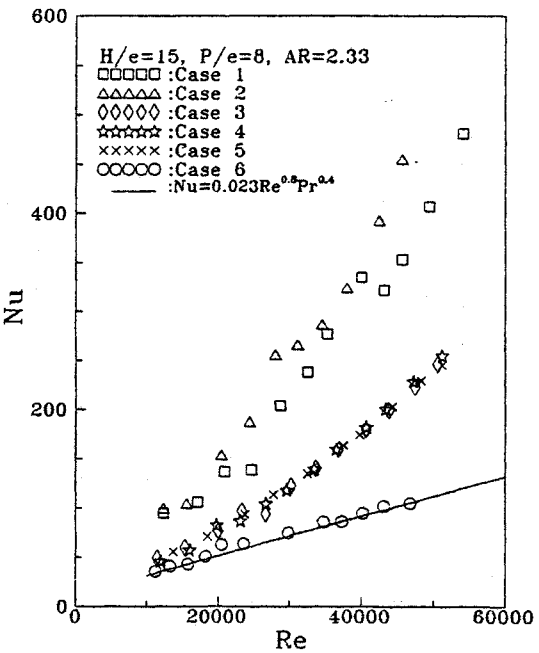

Fig. 4 Nusselt number

(Case 6) and compared with the results given in the literature, as shown in Figs. 3 and 4. The correlations for comparison includes Blasius equation (Kays and Crawford, 1993) for friction and Dittus-Boelter equation (1930) for heat transfer. All of these equations provide good representations of the data for a fully developed gas flow in smooth rectangular duct. It can be seen from these figures that the present fully

developed Nusselt numbers and friction factors of Case 6 compare well with the previous correlations. A fairly satisfactory agreement in the above comparison has confirmed that the experimental procedure employed is adequate and the results obtained are reliable. Figure 3 shows the friction factors for different rib shapes in Fig. 2. The square-shaped geometry (Case 1) has the highest value because of its strongest turbulence mixing caused by the ribs. Figure 4 indicates that the Nusselt numbers in Cases 1 and 2 are much higher than the other cases. It is because the radial turbulent fluctuating components become more significant in the sharp square-and triangle-shaped geometries. Close inspection of this figure further shows that, being different from in Fig. 3, the heat transfer in Case 2 is highest. This effect might be caused by the fact that the highest radial directional turbulent kinetic energy occurs in a sharp triangle-shape geometry of Case 2 because the surface of the sharp rib maintains the inclined angle to the main stream flow. It is, in general, known that the radial direction turbulent kinetic energy is closely related to the increase in heat transfer (Hwang, 1998).

For the laminar smooth channel flow, the non-circular ducts such as equilateral triangular, square, and rectangular ducts have lower friction factors and heat transfer than the circular ducts (Holman, 1990). However, for the turbulent smooth channel flow, the non-circular tubes including the present duct have almost same values with the circular tubes. This phenomenon is attributed to the fact that the increases in the friction factor and heat transfer are dependent upon fluid molecular properties in laminar flow regime, however, those are dependent upon the size of fluid element and radial direction turbulent kinetic energy in turbulent flow regime. Nusselt numbers non-dimensionalized by the smooth channel are indicated in Fig. 5. For a comparison, Hwang's data (1988) is involved. The deviation between Case 1 and Hwang's study increases with Re. It is because of the difference in the channel to rib height ratio. Around $Re=$ 10,000, Case 1 approaches to Hwang's data. This phenomenon is attributed to the fact that at the

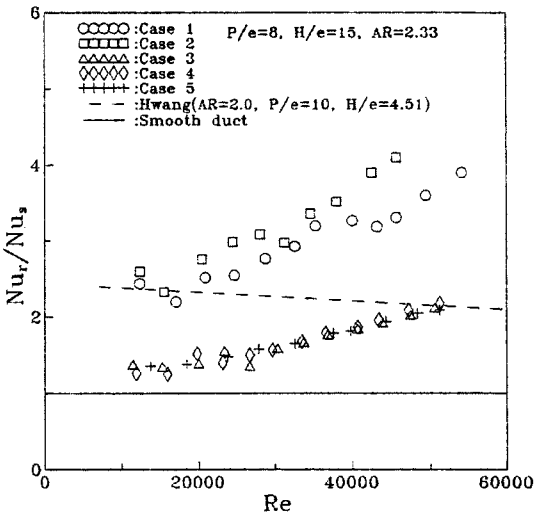

Fig. 5 Normalized Nusselt number

lower Reynolds number, the effect of the roughness on heat transfer becomes less. For the results of roughened surfaces to be most useful, general correlations are necessary for both the friction factor and heat transfer coefficient which cover a wide range of parameters. In fully developed turbulent flow, theoretical approaches to the problem of momentum transfer in smooth and rough tubes have been available for many years. These approaches are based on a similarity consideration. The surface is said to have geometrically similar roughness if the geometry of its roughness is the same in all aspects.

For example, sand grain roughness is a geometrically similar roughness. With repeated-rib roughness, for a given flow attack angle, rib shape and pitch-to-height ratio, tests with a different height-to-hydraulic diameter ratio represent geometrically similar roughness. However, when the values of P/e, flow attack angle or rib cross-section are varied, the surfaces are not geometrically similar. The surface which is not geometrically similar will require modifications to the roughness and heat transfer functions found by similarity consideration. Considering friction factors for geometrically similar roughness, the basic assumptions are the velocity defect law and the law of the wall. The first of these implies, for turbulent flow in a channel, the existence of a region away from the immediate vicinity of the

wall, where the direct effect of viscosity and roughness on the core flow is negligible. The law of the wall implies the existence of a region close to the wall. The velocity defect law and the law of the wall are combined to give Eq. (6):

$$U/U^*=2.5\ln(y/e)+Re^+(e^+) \qquad (6)$$

where U^* is the friction velocity. Based on these analysis, Nukuradse developed the friction similarity law for a sand-grain roughness surface shown in Eq. (7) by assuming Eq. (6) for the entire cross-section:

$$Re^+(e^+)=(2/f_r)^{1/2}+2.5\ln(2e/De)+3.75 \qquad (7)$$

where e^+ is the roughness Reynolds number and f_r is the friction factor obtained from the static pressure difference on the rough wall (Han, 1984). The roughness function Re^+ is a general function determined empirically for each type of geometrically similar roughness. The roughness function for Nikuradse's sand-grain roughness has the constant value 8.48 when e^+ is greater than 70; i.e. in completely rough regime, Re^+ does not depend on e^+. However, it is expected to be different for different geometrical roughness configurations. Figure 6 shows the roughness function against roughness Reynolds number, varying the rib shape in Fig. 2. For a comparison, the roughened parallel plates dealt by Han et al. (1978) are included. They are little lower than the present work because of the difference in the channel geometry. Dippery and Sabersky (1963) developed a heat transfer similarity law for a sand-grain roughness surface for the entire cross-section as follows:

$$\frac{f_r/(2St)-1}{(f_r/2)^{1/2}}+Re^+=He^+(e^+, \mathrm{Pr}) \qquad (8)$$

where St is $Nu/(Re\ Pr)$ and He^+ is heat transfer function. There are two methods of calculating the heat transfer coefficient of rib-roughened surfaces. First the heat transfer coefficient can be based on the projected area of the heat transfer surface; alternatively, the heat transfer coefficient can be based on the total area of the heat transfer surface including the rib area. When P/e is large, this effect is small. However, for a small value of P/e, the ribs constitute an appreciable fraction of the total area. Since metallic ribs are glued in this study, they maintain a temperature different from that of the floor plate. For this reason, the correlations for heat transfer coefficients are based on the projected area. In practice, the choice of the particular equation to use, either based on the total area or projected area depends upon the rib construction. If the rib is totally thin strip made of low conductivity material or when the rib is glued on the floor plate, the latter should be used. However, when the rib is a thick high conductivity material, the former is preferred.

The variation of heat transfer coefficient (He^+) against Reynolds number is shown in Fig. 7. The

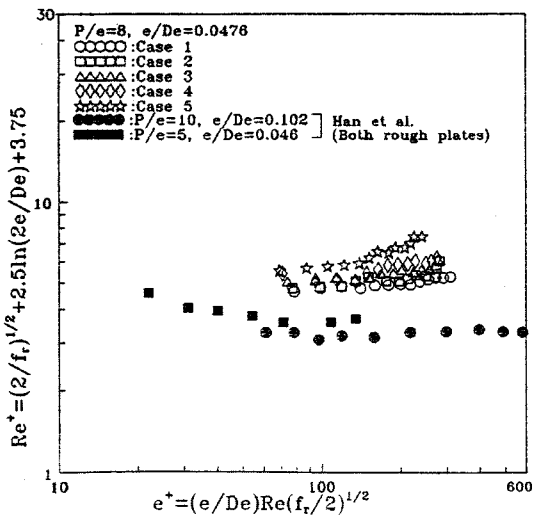

Fig. 6 Roughness function

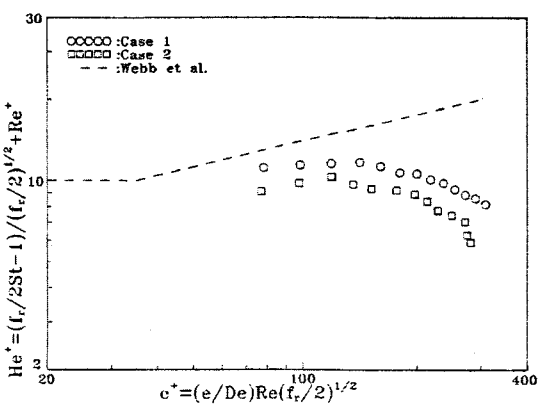

Fig. 7 Heat Transfer coefficient

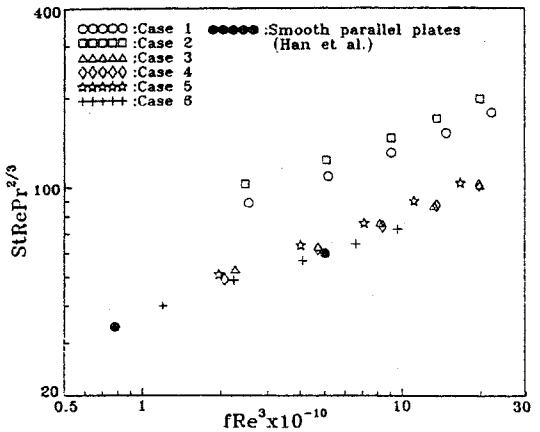

Fig. 8 Performance comparison

data of the roughened circular tube by Webb et al. (1971) is involved. On contrary to the roughened circular tube, heat transfer coefficient (He^+) decreases with increasing roughness Reynolds number (e^+). It may be due to the fact that the roughened circular tube (Webb et al., 1971) has the entire surface of a duct roughened and heated.

Mack and Rohsenow (1974) suggested a method to compare the performance of the different types of roughened surface. In Fig. 8, the horizontal axis is proportional to the pumping power per unit heat exchanger volume. The vertical axis represents the NTU, hA_s/mCp per unit volume for the same fluid at same temperature levels. Case 2 gives the highest heat transfer performance. For the smooth one, the rectangular duct has almost the same performance with the parallel plates.

4. Conclusion Remarks

(1) The square-shaped roughness geometry (Case 1) has the highest value in friction factor, meanwhile the triangle-shaped geometry (Case 2) has the highest value in heat transfer.

(2) Contrary to the roughened circular tube, the heat transfer coefficient (He^+) decreases with increasing roughness Reynolds number (e^+).

(3) Case 2 gives the highest heat transfer performance, and for the smooth one, the rectangular duct has almost the same performance with the parallel plates.

Acknowledgement

This work was supported by the Brain Korea 21 project

References

Arman, B. and Rabas, T. J., 1992, "Disrup tion Shape Effects on the Performance of Enhanced Tubes with the Separation and Re attachment Mechanism," *ASME Symposium*, Vol. HTD-202, ASME, NY, pp. 67~76.

Cope, W. F., 1941, "The Friction Factor and Heat Transfer Coefficients of Rough Pipes," *Proc. Inst. Mech. Engrs* 145, pp. 99~105.

Dipprey, D. F. and Sabersky, R. H., 1963, "Heat and Momentum Transfer in Smooth and Rough Tubes at Various Prandtl Number," *Int. J. Heat Mass Transfer*, Vol. 6, pp. 329~353.

Dittus, F. W. and Boelter, L. M. K., 1930, Univ. of California, Berkeley, Publications on Engineering, Vol. 2, p. 443.

Han, J. C., 1984, "Heat Transfer and Friction Factor in Channels With Two Opposite Rib-Roughened Walls," *J. of Heat Transfer*, Vol. 106, No. 4, pp. 774~781.

Han, J. C., Glicksman, L. R. and Rohsenow, W. M., 1978, "An Investigation of Heat Trans fer and Friction Factor for Rib-Roughened Surfaces," *Int. J. Heat Mass Transfer*, Vol. 21, pp. 1143~1156.

Hijikata, K. and Mori, Y., 1987, "Fundamental Study of Heat Transfer Augumentation of Tube Inside Surface by Cascade Smooth Turbulence Promoters and Its Application to Energy Conversion," *Warme-und-Stoff bertragung*, Vol. 21, pp. 115~124

Holman, J. P., 1990, *Heat Transfer*, Mc Graw-Hill Book Co., pp. 285-299.

Hwang, J. J., 1998, "Heat Transfer-Friction Characteristics Comparison in Rectangular Ducts with Slit and Solid Ribs Mounted on One Wall," J. Heat Transfer, Vol. 120, pp. 709~716.

Kays, W. M. and Crawford, M. E., 1993, *Convective Heat and Mass Transfer*, 3rd Ed.

McGraw-Hill, New York.

Kline, S. J. and McClintock, F. A., 1953, "Describing Uncertainties on Single Sample Experiments," *Mechanical Engineering*, Vol. 57, pp. 3~8.

Kwon, H. J., Wu, S. J. and Cho, H. H., 2000, "Effects of Discrete Rib-Turbulators on Heat/Mass Transfer Augumentation in a Rec tangular Duct," *Trans. KSME (B)*, Vol. 24, No. 5, pp. 744~752.

Mack, W. M. and Rohsenow, W. M., 1974, "Evaluation of the Heat Transfer Performance of Three Enhanced Surface Heat Exchanger Performance Comparison Method," Report No. DSR 74590-86, Heat Transfer Lab., Dept. of Mech. Engng, MIT.

Nikuradse, J., 1950, "Laws for Flow in Rough Pipes," *NACA TM* 1292.

Nunner, W., 1958, "Heat Transfer and Pres sure Drop in Rough Tubes," *AERE Lib/Trans.* 786.

Siegel, R. and Howell, J. R., 1981, *Thermal Radiation Heat Transfer*, 2nd ed. McGraw-Hill, New York.

Webb, R. L., Eckert, E. R. G. and Gold stein, R. J., 1971, "Heat Transfer and Friction in Tubes with Repeated-Rib Roughness," *Int. J. Heat Mass Transfer*, Vol. 14, pp. 601~617.